Fast and slow dynamics of the cytoskeleton

LINHONG DENG[1,2]*, XAVIER TREPAT[1], JAMES P. BUTLER[1], EMIL MILLET[1], KATHLEEN G. MORGAN[3,4], DAVID A. WEITZ[5] AND JEFFREY J. FREDBERG[1]

[1]Program in Molecular and Integrative Physiological Sciences, Harvard School of Public Health, Boston, Massachusetts 20115, USA
[2]Bioengineering College, Chongqing University, Chongqing 400044, China
[3]Boston Biomedical Research Institute, Watertown, Massachusetts 02472, USA
[4]Department of Medicine, Harvard Medical School, Boston, Massachusetts 20115, USA
[5]Department of Physics, Harvard University, Cambridge, Massachusetts 02138, USA
*e-mail: ldeng@hsph.harvard.edu

Published online: 9 July 2006; doi:10.1038/nmat1685

Material moduli of the cytoskeleton (CSK) influence a wide range of cell functions[1–3]. There is substantial evidence from reconstituted F-actin gels that a regime exists in which the moduli scale with frequency with a universal exponent of 3/4. Such behaviour is entropic in origin and is attributable to fluctuations in semiflexible polymers driven by thermal forces[4–7], but it is not obvious *a priori* that such entropic effects are responsible for the elasticity of the CSK. Here we demonstrate the existence of such a regime in the living cell, but only at high frequencies. Fast events scaled with frequency in a manner comparable to semiflexible-polymer dynamics, but slow events scaled with a non-universal exponent that was systematically smaller than 3/4 and probably more consistent with a soft-glass regime[8,9]. These findings strongly suggest that at smaller timescales elasticity arises from entropic fluctuations of a semiflexible-filament network, whereas on longer timescales slow (soft-glass-like) dynamics of a different origin prevail. The transition between these two regimes occurred on timescales of the order of 0.01 s, thus setting within the slow glassy regime cellular events such as spreading, crawling, contracting, and invading.

A major constituent of the CSK is F-actin. Reconstituted F-actin gels *in vitro* show clear evidence of semiflexible-polymer network dynamics[6,7,10,11]. At lower frequencies, f, network elasticity is frequency-independent, but at higher frequencies the elasticity approaches a regime where it increases as $f^{3/4}$, consistent with the theoretical prediction[4,12–16]

$$G^*(f) \sim (\rho\kappa l_p/15)(4i\zeta\pi f/\kappa)^{3/4}, \qquad (1)$$

where $G^*(f)$ is the complex modulus, ρ, κ, ζ, and l_p are the density, bending stiffness, lateral drag coefficient, and persistence length of actin filaments in the gel, respectively, and $i^2 = -1$; here we have suppressed a small newtonian viscosity that contributes little except at very high frequencies. Equation (1) is a consequence of filament entropy wherein elasticity at high frequencies becomes dominated by lateral bending fluctuations of semiflexible filaments (F-actin) driven by thermal perturbations[4,12,15,16]. This behaviour has been found to hold in a variety of F-actin solutions over wide ranges of actin concentration, extent of entanglement, and gel crosslinking[14].

Dynamics of this type have yet to be observed in the living cell[4–7]. Moreover, in the highly crosslinked and short-filament networks of the cell, and under the appreciable pre-stress to which the cell is subjected[17], it is not obvious that entropic effects can be responsible for the elasticity. Indeed, in a variety of cell types, as well as in F-actin gels that are pre-stressed and crosslinked by filamin, dynamics of a rather different type have recently been reported[8,9,18–20].

To fill this gap and to assess the existence of a regime comparable to that suggested by equation (1), here we report rheological properties of the freshly isolated living airway smooth muscle (ASM) cell. Compared with the CSK of the smooth muscle cell passaged in culture, that of the freshly isolated smooth muscle cell has substantially more organization[21], higher density of contractile filaments, more smooth-muscle-specific actin-binding proteins (h-caldesmon, h-1 calponin, and sm22) and myofilament bundles, but fewer microtubules (K.M., personal communication). In addition, the freshly dissociated ASM cell has a long worm-like shape that more closely approximates the morphology of the ASM cell *in situ*[22,23] (Fig. 1a). In these cells, we measured G^* as described in the Methods section. Collectively, data spanned baseline, relaxation, and contraction conditions, and spanned four orders of magnitude in frequency.

Variability of G' (the real part of G^*) from bead-to-bead was extensive and approximated a log-normal distribution, as is found in other cell preparations[19,24]. Nonetheless, from bead-to-bead the frequency dependence of G' was highly consistent (Fig. 2a). G'' (the imaginary part of G^*) exhibited a comparable degree of variability and increased systematically with frequency (Fig. 2b). Although both G' and G'' were highly variable across cells, the variability of their ratio (loss tangent, η) was slight (Fig. 2b, inset). Pooled data for G' (geometric mean and geometric standard error) increased

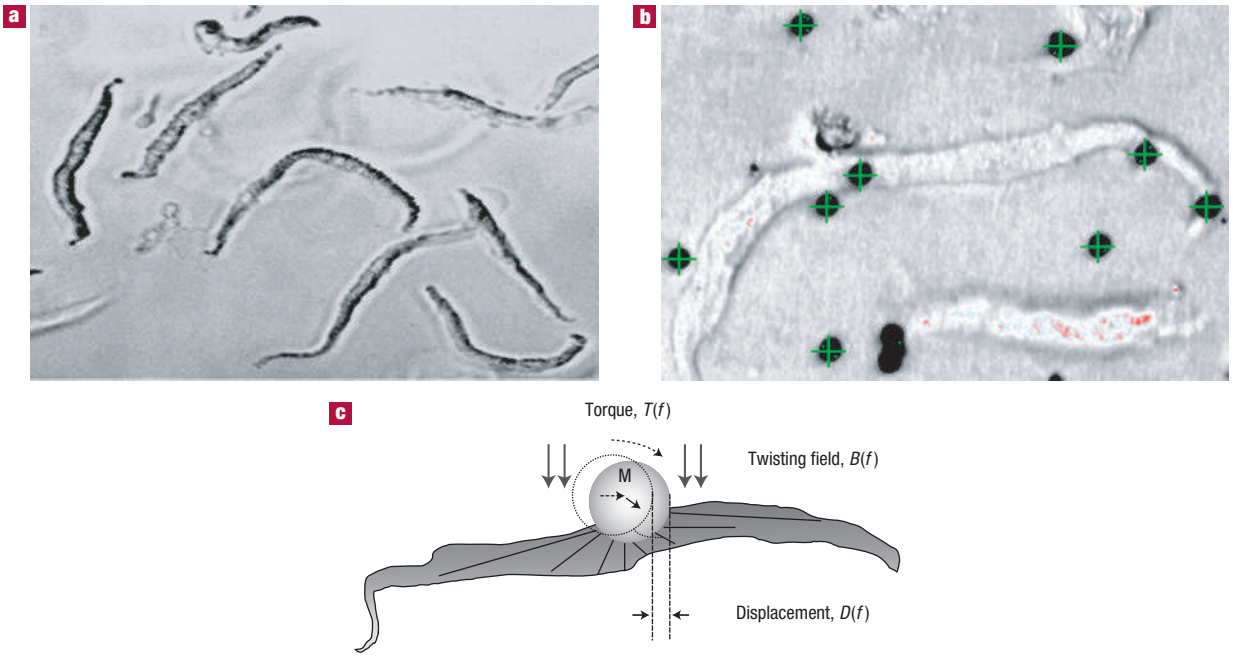

Figure 1 Freshly isolated bovine trachea smooth muscle cells, with bound beads, and the twisting cytometry method. a, Photomicrograph of freshly isolated bovine trachea smooth muscle cells (typically 150 to 200 micrometres long) adhered to a poly-L-lysine substrate. Note the typical long worm-like appearance. 4–5 h after first settling on the substrate, healthy cells usually established firm attachment with various contact points. **b**, Bovine trachea smooth muscle cells with beads attached. RGD-coated ferrimagnetic beads were introduced and allowed to bind to the integrin receptors on the surface of the adherent cells (20 min). A charge-coupled device camera was used to identify each bead, which was then marked with a cross-hair determined by the centre position of its image. **c**, Schematic diagram of the magnetic twisting cytometry method in which the bead was oscillated at a frequency, *f*, from 0.09 to 1,000 Hz by a torque, *T*, caused by a sinusoidal magnetic field, *B*, of 20 G magnitude at *f*. The resultant sinusoidal displacement, *D*, of the bead was measured from the recorded bead positions during the oscillation.

slowly with frequency at frequencies below 100 Hz, but much more rapidly at frequencies greater than 100 Hz (Fig. 3). Compared with the frequency dependence of G', that of G'' was smaller at lower frequencies but higher at higher frequencies.

On a cell-by-cell basis, we fitted these data in the complex plane (see the Methods section) to the relationship $G^*(f) = A(if)^\alpha + B(if)^\beta$. G' data were well represented by the best fit, but G'' data at lower frequencies fell systematically above and had weaker frequency dependence than indicated by the best fit (Fig. 3, solid lines); similar discrepancies have been reported in bronchial epithelial cells, macrophages and neutrophils[24], and are a signature of soft glassy materials that are ageing[25–28].

Although our technology is limited to frequencies below 1 kHz, our data were sufficient to resolve the exponents α and β and put relatively narrow bounds on their values (see the additional comments on statistical tests in the Supplementary Information). Across the cell population ($N = 64$), the distributions of α and β were approximately normal (Fig. 4). The mean of α was 0.05 (95% confidence interval 0.04–0.06) and was different from zero ($p < 0.00001$); as described below, this implies that at low frequencies the system did not approach a hookean limit. The mean of β was 0.75, (95% confidence interval 0.69–0.79) and was different from unity ($p < 0.00001$); as described below, this implies that at high frequencies the system did not approach a newtonian limit. Indeed, setting β to unity degraded the fit and adding a newtonian viscous term led to a result that was physically unrealizable (see the Supplementary Information).

Distinct values of α and β imply that the rheology in these cells was characterized by two distinct regimes. In excess of 100 Hz, the complex modulus approached $f^{0.75}$, a scaling behaviour consistent with that predicted by the theory of semiflexible polymers[4,12,15,16]. Such high-frequency dynamics have not been noted previously in the living cell although, in retrospect, a hint of such behaviour is evident in cells passaged in culture[24]. In contrast, at lower frequencies semiflexible-polymer dynamics became subdominant, with the complex modulus scaling as $f^{0.05}$. This exponent was non-universal, as shown below, and was systematically smaller than that observed in ASM cells passaged in culture, where, typically, $0.1 < \alpha < 0.3$ (refs 8,17,24,29), but is comparable to that found in intact activated ASM strips (data not shown).

G^* increased with contractile activation (KCl, 80 mM) and decreased with relaxation (dibutyryl cAMP, 1 mM) (Supplementary Information, Fig. S1). The exponent β was not influenced by relaxation, but decreased during contraction from 0.75 to 0.64 (95% confidence interval 0.57 to 0.71) (Supplementary Information Fig. S2, top), suggesting that contraction altered the qualitative nature of the high-frequency behaviour, whereas relaxation did not. Values of β smaller than 3/4 are consistent with behaviour observed in pre-stressed F-actin gels[14]. Indeed, pre-stress in cells[17,30] and in filamin-crosslinked gels[20] is known to be a major determinant of dynamics in the slow glassy regime, but the role of pre-stress in the fast regime could not be addressed in the experiments described here and remains a major open question. The exponent α decreased slightly during cell contraction, but during cell relaxation it increased from 0.05 to 0.08 (95% confidence interval 0.06 to 0.09) (Supplementary Information, Fig. S2, bottom).

Why should material moduli at low frequencies scale with a weak non-universal exponent? When taken together with other observations, such behaviour has been taken as strong evidence

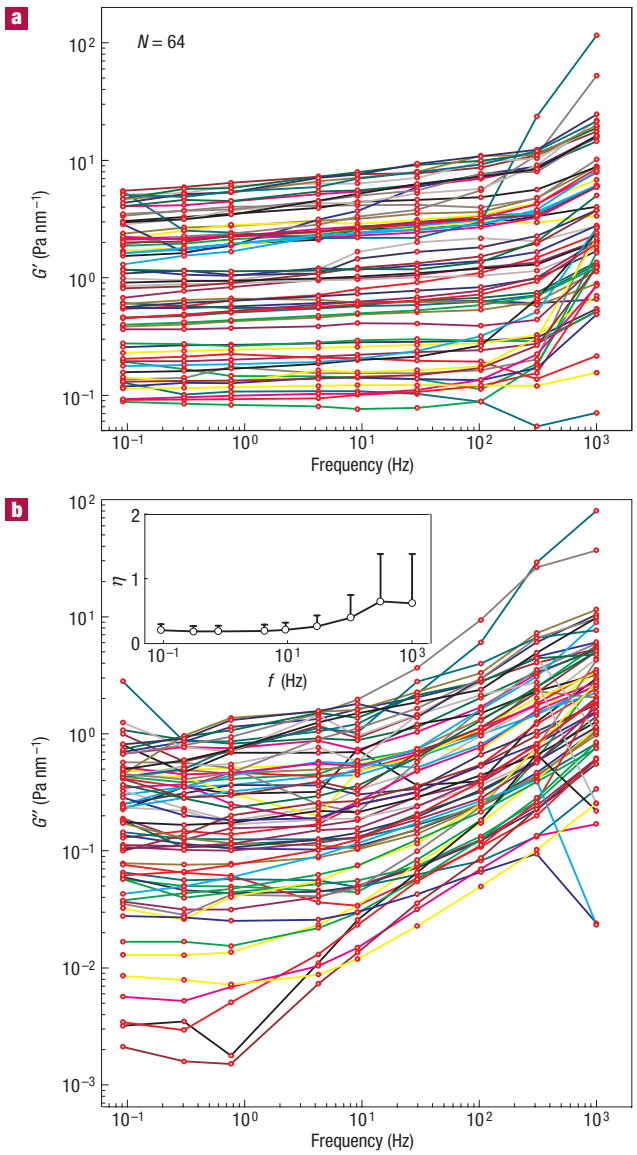

Figure 2 Storage modulus (G') and loss modulus (G'') as a function of frequency for all beads measured ($N = 64$). a,**b**, G' (**a**) and G'' (**b**) varied broadly across beads, approximately log-normally. However, the hysteresivity or loss tangent $\eta = G''/G'$ varied little across beads, and only weakly with frequency (inset, mean ± standard deviation).

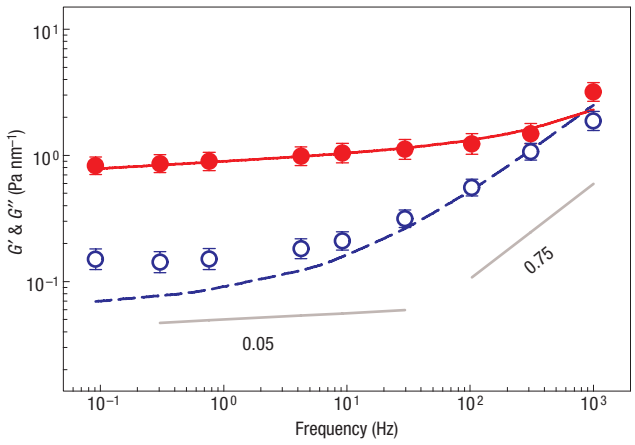

Figure 3 Pooled data of G' (red, filled circles) and G'' (blue, open circles) from all individual beads, together with the average two-term power-law fit (solid lines). The data presented are the geometric mean, and the corresponding error bars represent the geometric standard error defined as the standard error of the data set in logarithmic space. The solid lines represent the two-term power-law fit with geometric means of A and B, and arithmetic means of α and β. This graph clearly demonstrates the two regimes of frequency dependence measured in the freshly isolated ASM cell. At lower frequencies, the moduli increased with frequency as a weak power law with exponent 0.05. At higher frequencies, the moduli increased as a stronger power law with exponent 0.75. The transition occurred at about 100 Hz. The straight grey lines denote slopes of 0.05 and 0.75.

for non-equilibrium behaviour and, in particular, a glassy regime of CSK dynamics has been suggested[8,9]. The ability of a liquid to form a glass is related to slowly relaxing degrees of freedom which, under certain conditions, may persist out of equilibrium[31]. By the term 'slow', here we mean processes that decay more slowly than any exponential, such as logarithmic or weak power-law decay. In various inert glassy systems, slow degrees of freedom have been attributed to a variety of possibilities, including slow motions of polymer chains constrained by chemical crosslinks, entanglements or loops, slow turnover of covalent or non-covalent bonds connecting constituent structures to form a bond network, slow relaxation towards energetically favourable configurations, and slow structural rearrangements arising from crowding, caging, and jamming[32–35]. Despite this variety, traditional glassy systems share one feature in common: slow localized inelastic rearrangements, and the applicability of such a point of view is justified by the universality of the phenomenology[25,31]. In the living cell, none of the above can be ruled out and, as we suggested previously, ATP-dependent rearrangements might modify CSK microconfigurations and thereby provide an alternate means of exploring new network configurations[9]. ATP hydrolysis can drive both conformational changes and polymerization/depolymerization cycles of CSK proteins, either or both of which could conceivably resolve constraints and drive structural rearrangements.

Consistent with that physical picture[9,25,36], but in contrast with equation (1), the complex modulus of the ASM cell passaged in culture has been shown to go as[8,24]

$$G^*(f) \sim G_0 \Gamma(1-\alpha)\{i2\pi f/\Phi_0\}^{\alpha}, \qquad (2)$$

where $\Gamma()$ is the gamma function, and G_0 and Φ_0 are scale factors for stiffness and frequency, respectively, and again we have suppressed a small newtonian viscosity.

We suggest that equations (1) and (2) describe the high-frequency $[B(if)^{3/4}]$ and low-frequency $[A(if)^{\alpha}]$ terms of the best fit, respectively. As regards low-frequency behaviour of the CSK[8,18,19,24,29] and equation (2), the non-universal exponent α becomes a continuous measure of proximity of the CSK to solid-like ($\alpha = 0$; $G'' = 0$) versus fluid-like ($\alpha = 1$; $G' = 0$) behaviours. In contrast, the observation of G^* approaching $f^{3/4}$ at higher frequencies suggests the emergence of entropic dynamics associated with semiflexible polymers and in this report it is identified for the first time in living cells. Despite uncertainties in the values of the various factors in equation (1), values found in the literature yield a prefactor, B, that is within an order of magnitude of that which was observed experimentally; this correspondence represents independent evidence that the fast regime indeed arises from dynamics of semiflexible polymers.

Therefore, we conclude that in the living cell the dynamics of semiflexible polymers and soft glasses coexist, but each dominates

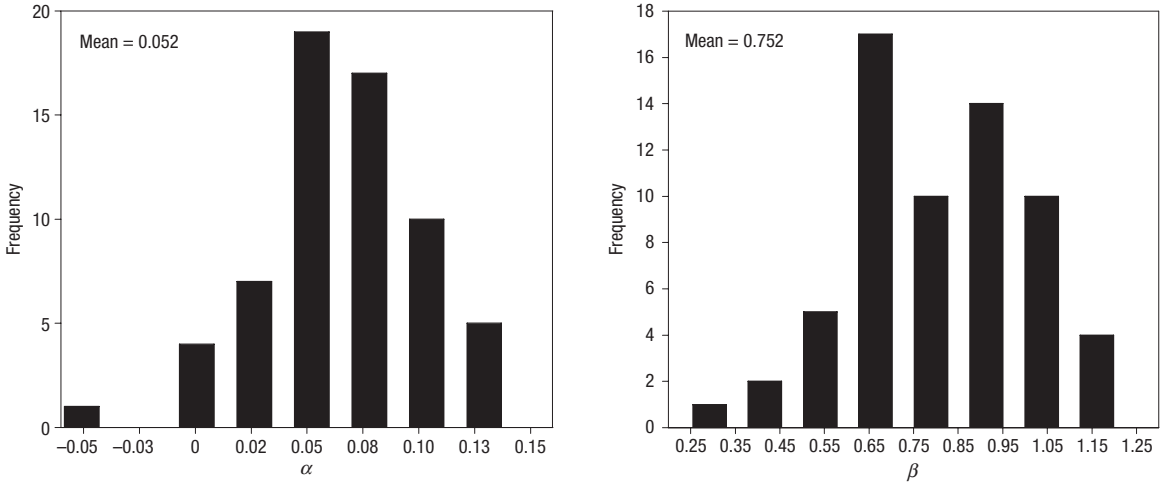

Figure 4 Distributions of the two exponents, α and β, that characterize the two distinct regimes of CSK dynamics. These were both approximately normal. The mean and standard deviation of α were 0.05 and 0.036, respectively (95% confidence interval 0.04–0.06). The mean and standard deviation of β were 0.75 and 0.19 (95% confidence interval 0.69–0.79). A Student's *t*-test verified that α was significantly different from zero ($p < 0.00001$), and β was significantly different from unity ($p < 0.00001$), but not different from 0.75 ($p > 0.5$).

on different timescales. On shorter timescales (higher frequencies), there is insufficient time for inelastic structural rearrangements and, as such, relatively fast thermal fluctuations drive bending of semiflexible CSK filaments and determine material properties of the CSK. In this fast regime, as crosslink density increases, entropic contributions to the elasticity diminish relative to the enthalpic contributions[14]. However, on longer timescales (lower frequencies) slow inelastic rearrangements of the CSK prevail[8,9], and the effects of thermally driven filament bending become subdominant. Such an interpretation implies sustained departure from thermodynamic equilibrium and is consistent with the finding that in the living ASM cell on longer timescales the generalized Stokes–Einstein relationship breaks down[9].

It was not obvious *a priori* that entropic effects could be responsible for cell elasticity. The results presented here are the first evidence to suggest that they are. As these results resemble so clearly what is seen in simple reconstituted but crosslinked actin networks, they also strongly support the idea that the bead-twisting probe we used is most sensitive to the cytoskeletal actin network. All prior measurements in other cell systems show power-law responses with non-universal exponents in the range 0.1–0.3 (refs 8,17–19,24,29), and it was not clear from those measurements if a distinct high-frequency regime might exist. The results presented here show that such a regime does exist and that its exponent is 3/4.

As such, data reported here unify within the same cell these two distinct schools of thought, and suggest that the transition between regimes occurs on timescales of the order of 10^{-2} s. Accordingly, these data set within the slow glassy regime timescales typical of integrated mechanical events of the cell such as spreading, crawling, contracting, and invading.

METHODS

All chemical reagents, standard buffer solutions, and media were purchased from Sigma unless stated otherwise.

PREPARATION OF INTACT LIVING CELLS

Single ASM cells were freshly isolated from bovine trachea by enzymatic digestion, which was adopted from a previously described method[23]. Briefly, a bovine trachea was obtained from an abattoir and transported to the laboratory within 2 h of excision. Before use, the tissue was maintained at 4 °C in an oxygenated (95% O_2 and 5% CO_2) buffer containing 1:1 Hank's balanced salt solution and Dulbecco's modified Eagle's medium, and 1,000 Unit ml^{-1} of penicillin and streptomycin. Subsequently, in constantly oxygenated Krebs solution (120 mM NaCl, 5.9 mM KCl, 1.2 mM NaH_2PO_4, 25 mM $NaHCO_3$, 11.5 mM dextrose, 1 mM $CaCl_2$, and 1.4 mM $MgCl_2$), 50 mg wet weight of ASM was dissected from the trachea and cut into 2 × 3 mm pieces. The tissue was then transferred into a siliconized, that is, coated with SigmaCote, flask containing an enzymatic digestion solution. The digestion solution consisted of 182 Unit ml^{-1} Type 2 collagenase (Worthington), 3.0 Unit ml^{-1} Grade II elastase (Roche Diagnostics), and 5,000 Unit ml^{-1} Type II-S soybean trypsin inhibitor in a Ca^{2+} and Mg^{2+} free buffer consisting of 137 mM NaCl, 5.4 mM KCl, 5.6 mM dextrose, 4.2 mM $NaHCO_3$, 0.42 mM Na_2HPO_4, 0.44 mM KH_2PO_4, and 0.075% bovine serum albumin. The tissue was incubated in this digestion solution in a shaking water bath (9.6 cycles min^{-1}) at 34 °C and oxygenated atmosphere for 40 min. The dissociated cells were filtered through nylon gauze (526 μm mesh size) and rinsed with 10 ml of the Ca^{2+} and Mg^{2+} free buffer. More cells may be harvested by repeatedly incubating the remaining tissue in the digestion solution, but in a progressively reduced concentration of collagenase.

Dissociated cells were poured over glass coverslips or 96 wells coated with poly L-lysine and incubated for 40 min on ice. Cell viability was verified by KCl-induced contraction of sample cells in each batch of harvested cells.

Because these cells were adherent on a rigid substrate at the time of measurement, all contractions were isometric. Although we did not use traction microscopy to measure contractile stresses, as we have in our previous work[17,30], these cells probably do maintain appreciable axial tension.

MEASUREMENT OF THE DYNAMIC MODULUS

To probe the microrheology of CSK, ferrimagnetic beads (4.5 μm diameter) were coated with a synthetic peptide containing the Arg–Gly–Asp (RGD; Peptite 2000, Integra Life Sciences) sequence and allowed to adhere to the apical cell surface. These beads become tightly tethered to the F-actin CSK through transmembrane integrin receptors, mostly $\alpha_5\beta_1$; these receptors bind to the RGD ligand in the extracellular domain and the focal adhesion and actin filaments in the intracellular domain[1,8,24,29,37–39] (Fig. 1b). We then measured the complex modulus as a function of frequency by applying an oscillatory magnetic field and measuring the resultant oscillatory bead motions with light microscopy[24,37] (Fig. 1c). When the oscillatory magnetic field of frequency f was applied to the bead, it resulted in an oscillatory torque $\tilde{T}$, where the tilde overbar denotes the Fourier domain. The induced lateral displacement of the

bead, $\tilde{D}$, was measured using a charge-coupled device camera attached to an inverted optical microscope (Leica Microsystems). The complex modulus is then simply

$$G^*(f) = \tilde{T}/\tilde{D}.$$

G^* measured in this way has units of torque per unit bead volume per unit bead displacement, or Pa nm^{-1}. This can be converted to familiar material moduli with the use of a length scale derived from a model of cell deformation[40], but to avoid model-dependent assumptions here we report all data in primary measurement units of Pa nm^{-1}.

DATA ANALYSIS AND FITTING

Denote the complex modulus of the nth bead at frequency f_m by $G_n^*(f_m)$. For each bead (that is, for each n), the two-term power-law model, $G^*(f) = A(if)^\alpha + B(if)^\beta$ was fitted to these data by minimizing $\sum_{m=1,M} |\log G^*(f_m) - \log G_n^*(f_m)|^2$ with respect to the parameters A, B, α, β. M is the number of frequencies used, typically 9, spanning 0.1 Hz to 1 kHz in half log increments. The distributions of the parameters obtained from this bead-by-bead fit were examined statistically. R project, a freely available statistical software package (www.r-project.org), was used to fit the model to the data and for statistical analysis. One-way analysis of variance, and Student's t-test were used to examine the differences in the parameters when compared among multiple conditions or between two conditions, respectively. Differences with $p < 0.05$ were considered statistically significant.

Received 17 February 2006; accepted 19 May 2006; published 9 July 2006.

References

1. Chicurel, M. E., Chen, C. S. & Ingber, D. E. Cellular control lies in the balance of forces. *Curr. Opin. Cell. Biol.* **10,** 232–239 (1998).
2. Discher, D. E., Janmey, P. & Wang, Y. L. Tissue cells feel and respond to the stiffness of their substrate. *Science* **310,** 1139–1143 (2005).
3. Janmey, P. A. & Weitz, D. A. Dealing with mechanics: mechanisms of force transduction in cells. *Trends Biochem. Sci.* **29,** 364–370 (2004).
4. Gittes, F., Schnurr, B., Olmsted, P. D., MacKintosh, F. C. & Schmidt, C. F. Microscopic viscoelasticity: Shear moduli of soft materials determined from thermal fluctuations. *Phys. Rev. Lett.* **79,** 3286–3289 (1997).
5. Morse, D. C. Viscoelasticity of concentrated isotropic solutions of semiflexible polymers. 2. Linear response. *Macromolecules* **31,** 7044–7067 (1998).
6. Gardel, M. L., Valentine, M. T., Crocker, J. C., Bausch, A. R. & Weitz, D. A. Microrheology of entangled F-actin solutions. *Phys. Rev. Lett.* **91,** 158302 (2003).
7. Gardel, M. L. *et al.* Elastic behavior of cross-linked and bundled actin networks. *Science* **304,** 1301–1305 (2004).
8. Fabry, B. *et al.* Scaling the microrheology of living cells. *Phys. Rev. Lett.* **87,** 148102 (2001).
9. Bursac, P. *et al.* Cytoskeletal remodelling and slow dynamics in the living cell. *Nature Mater.* **4,** 557–561 (2005).
10. Kas, J., Strey, H. & Sackmann, E. Direct imaging of reptation for semiflexible actin filaments. *Nature* **368,** 226–229 (1994).
11. MacKintosh, F. C., Kas, J. & Janmey, P. A. Elasticity of semiflexible biopolymer networks. *Phys. Rev. Lett.* **75,** 4425–4428 (1995).
12. Gittes, F. & MacKintosh, F. C. Dynamic shear modulus of a semiflexible polymer network. *Phys. Rev. E* **58,** R1241–R1244 (1998).
13. Gisler, T. & Weitz, D. A. Scaling of the microrheology of semidilute F-actin solutions. *Phys. Rev. Lett.* **82,** 1606–1609 (1999).
14. Gardel, M. L. *et al.* Scaling of F-actin network rheology to probe single filament elasticity and dynamics. *Phys. Rev. Lett.* **93,** 188102 (2004).
15. Morse, D. C. Viscoelasticity of tightly entangled solutions of semiflexible polymers. *Phys. Rev. E* **58,** R1237–R1240 (1998).
16. Morse, D. C. Viscoelasticity of concentrated isotropic solutions of semiflexible polymers. 1. Model and stress tensor. *Macromolecules* **31,** 7030–7043 (1998).
17. Stamenovic, D., Suki, B., Fabry, B., Wang, N. & Fredberg, J. J. Rheology of airway smooth muscle cells is associated with cytoskeletal contractile stress. *J. Appl. Physiol.* **96,** 1600–1605 (2004).
18. Alcaraz, J. *et al.* Microrheology of human lung epithelial cells measured by atomic force microscopy. *Biophys. J.* **84,** 2071–2079 (2003).
19. Desprat, N., Richert, A., Simeon, J. & Asnacios, A. Creep function of a single living cell. *Biophys. J.* **88,** 2224–2233 (2005).
20. Gardel, M. L. *et al.* Prestressed F-actin networks cross-linked by hinged filamins replicate mechanical properties of cells. *Proc. Natl Acad. Sci. USA* **103,** 1762–1767 (2006).
21. Draeger, A., Stelzer, E., Herzog, M. & Small, J. Unique geometry of actin-membrane anchorage sites in avian gizzard smooth muscle cells. *J. Cell Sci.* **94,** 703–711 (1989).
22. Bagby, R. M., Young, A. M., Dotson, R. S., Fisher, B. A. & McKinnon, K. Contraction of single smooth muscle cells from Bufo marinus stomach. *Nature* **234,** 351–352 (1971).
23. DeFeo, T. T. & Morgan, K. G. Responses of enzymatically isolated mammalian vascular smooth muscle cells to pharmacological and electrical stimuli. *Pflugers Arch.* **404,** 100–102 (1985).
24. Fabry, B. *et al.* Time scale and other invariants of integrative mechanical behavior in living cells. *Phys. Rev. E* **68,** 041914 (2003).
25. Sollich, P., Lequeux, F., Hebraud, P. & Cates, M. E. Rheology of soft glassy materials. *Phys. Rev. Lett.* **78,** 2020–2023 (1997).
26. Cates, M. E. & Sollich, P. in *Foams and Emulsions* (eds Sadoc, J. F. & Rivier, N.) 207–236 (Kluwer Academic, Dordrecht, 1999).
27. Mason, T. G., Gisler, T., Kroy, K., Frey, E. & Weitz, D. A. Rheology of F-actin solutions determined from thermally driven tracer motion. *J. Rheol.* **44,** 917–928 (2000).
28. Gopal, A. D. & Durian, D. J. Relaxing in foam. *Phys. Rev. Lett.* **91,** 188303 (2003).
29. Puig-de-Morales, M. *et al.* Cytoskeletal mechanics in adherent human airway smooth muscle cells: probe specificity and scaling of protein-protein dynamics. *Am. J. Physiol. Cell Physiol.* **287,** C643–C654 (2004).
30. Wang, N. *et al.* Cell prestress. I. Stiffness and prestress are closely associated in adherent contractile cells. *Am. J. Physiol. Cell Physiol.* **282,** C606–C616 (2002).
31. Bulatov, V. V. & Argon, A. S. A stochastic-model for continuum elastoplastic behavior. 2. A study of the glass-transition and structural relaxation. *Modelling Simul. Mater. Sci. Eng.* **2,** 185–202 (1994).
32. Weeks, E. R., Crocker, J. C., Levitt, A. C., Schofield, A. & Weitz, D. A. Three-dimensional direct imaging of structural relaxation near the colloidal glass transition. *Science* **287,** 627–631 (2000).
33. Mazurin, O. V. Theory of glass-transition—chemical-equilibria approach. *J. Non-Cryst. Solids* **129,** 259–265 (1991).
34. Kovacs, A. J., Aklonis, J. J., Hutchinson, J. M. & Ramos, A. R. Isobaric volume and enthalpy recovery of glasses. 2. Transparent multi-parameter theory. *J. Polym. Sci. Polym. Phys.* **17,** 1097–1162 (1979).
35. Chen, H. S. & Turnbull, D. Evidence of a glass–liquid transition in a gold–germanium–silicon alloy. *J. Chem. Phys.* **48,** 2560–2571 (1968).
36. Sollich, P. Rheological constitutive equation for a model of soft glassy materials. *Phys. Rev. E* **58,** 738–759 (1998).
37. Wang, N., Butler, J. P. & Ingber, D. E. Mechanotransduction across the cell surface and through the cytoskeleton. *Science* **260,** 1124–1127 (1993).
38. Deng, L., Fairbank, N. J., Fabry, B., Smith, P. G. & Maksym, G. N. Localized mechanical stress induces time-dependent actin cytoskeletal remodeling and stiffening in cultured airway smooth muscle cells. *Am. J. Physiol. Cell Physiol.* **287,** C440–C448 (2004).
39. Choquet, D., Felsenfeld, D. P. & Sheetz, M. P. Extracellular matrix rigidity causes strengthening of integrin-cytoskeleton linkages. *Cell* **88,** 39–48 (1997).
40. Mijailovich, S. M., Kojic, M., Zivkovic, M., Fabry, B. & Fredberg, J. J. A finite element model of cell deformation during magnetic bead twisting. *J. Appl. Physiol.* **93,** 1429–1436 (2002).

Acknowledgements

The authors would like to thank C. Gallant for her assistance in the adaptation of the cell isolation method. X.T. is supported by a postdoctoral fellowship from the Spanish Ministerio de Educación y Ciencia. This study was financially supported by NIH HL65960, HL33009 and HL31704.
Correspondence and requests for materials should be addressed to L.D.
Supplementary Information accompanies this paper on www.nature.com/naturematerials.

Competing financial interests

The authors declare that they have no competing financial interests.

Reprints and permission information is available online at http://npg.nature.com/reprintsandpermissions/